IOP Conf. Series: Materials Science and Engineering **311** (2018) 012004 doi:10.1088/1757-899X/311/1/012004

Smart reconfigurable parabolic space antenna for variable electromagnetic patterns

Sahil Kalra[1], Rituparna Datta[2], B.S.Munjal[3], and Bishakh Bhattacharya[4]

[1,4]Department of Mechanical Engineering, Indian Institute of Technology Kanpur, India
[2]Graduate School of knowledge Service Engineering, KAIST, South Korea
[3]Space Applications Centre, Indian space research organization, Ahmedabad, India
bishakh@iitk.ac.in

Abstract. An application of reconfigurable parabolic space antenna for satellite is discussed in this paper. The present study focuses on shape morphing of flexible parabolic antenna actuated with Shape Memory Alloy (SMA) wires. The antenna is able to transmit the signals to the desired footprint on earth with a desired gain value. SMA wire based actuation with a locking device is developed for a precise control of Antenna shape. The locking device is efficient to hold the structure in deformed configuration during power cutoff from the system. The maximum controllable deflection at any point using such actuation system is about 25mm with a precision of $\pm 100\mu$m. In order to control the shape of the antenna in a closed feedback loop, a Proportional, Integral and Derivative (PID) based controller is developed using LabVIEW (NI) and experiments are performed. Numerical modeling and analysis of the structure is carried out using finite element software ABAQUS. For data reduction and fast computation, stiffness matrix generated by ABAQUS is condensed by Guyan Reduction technique and shape optimization is performed using Non-dominated Sorting Genetic Algorithm (NSGA-II). The matching in comparative study between numerical and experimental set-up shows efficacy of our method. Thereafter, Electro-Magnetic (EM) simulations of the deformed shape is carried out using electromagnetic field simulation, High Frequency Structure Simulator (HFSS). The proposed design is envisaged to be very effective for multipurpose application of satellite system in the future missions of Indian Space Research Organization (ISRO).

1. Introduction

Antennas are the basic constituents of a satellite communication system. It acts as a transferring medium of radio waves between two ground stations commonly known as uplink and downlink. Depending upon frequency band, polarization, field of application and mode of operation, antennas can be categorized into various groups and sub groups as shown in Fig. 1. Each sub group in Fig. 1 has its own type depending upon the characteristics of service and functionality. Among this group, parabolic reflectors are most common for space applications.

Using the concepts of Geometric Optics (GO) it can easily be proved that for a perfect parabolic surface, all rays covers equal distance from focus to the aperture plane. Hence, far field radiations pattern of such reflector produces a similar pencil beam along focus of the parabola. However, the bandwidth (HPBW) at variable frequencies / wavelength shows the difference. The band width is inversely proportional to the operational frequency. For example, increasing the frequency by 10% reduces the HPBW by the same amount as shown in Fig.2. One of the categories of parabolic reflectors are shaped reflectors which have relatively better HPBW. However, their shape is unique corresponding to the geographical area to scan and the gain in given direction is also fixed. Hence, for

space applications there is high demand of a reflector whose gain and footprints can actively be steered and shaped.
In the previous studies reconfigurable parabolic antennas actuated using Piezoelectric actuators were studied by researchers [3, 4]. Most of the past studies were performed by considering assumption which cannot be verified experimentally [1-2] especially in the space environment. However, the space environment conditions require non-degradable actuators with low power consumption.
In order to overcome these challenges, we have demonstrated a Shape Memory Alloy (SMA) actuated single feed antenna system which can change the gain of radiation pattern and actively change the footprints. A C-band parabolic reflector made of flexible polycarbonate Lexan material (E = 1.5GPa) (shown in Fig.12) is presented for the analysis. An attempt has been made to present a unique concept for the first time as a dedicated locking device which is based upon the requirement to lock the shape of antenna even though power supply is cut off from the system [5]. As continuous power supply from spacecraft may destabilize the satellite in Roll, Pitch & Yaw axes, hence the need has been felt for such innovation. The effect of shape change of antenna on EM pattern is also studied in this paper. Thereafter, we have presented a multi-objective Genetic Algorithm (GA) based approach to minimize the voltage requirements and minimizing the error between the desired and achieved shape.

Frequency Basis: 1. VLF (3-30KHz) 2. LF (30-300KHz) 3. HF (3-30MHz) 4. VHF (30-300MHz) 5. UHF (300-3000 MHz) 6. SHF (3-30GHz) 7. EHF (30-300GHz)	**Aperture Antennas:** 1. Wire Antennas 2. Horn Antennas 3. Parabolic reflective Antenna 4. Cassegrain Antenna
Polarization Basis: 1. Linearly Polarized Antenna 2. Circularly Polarized Antenna	**Radiation Pattern Basis:** 1. Isotropic Antenna 2. Omnidirectional Antenna 3. Directional Antenna 4. Hemispherical Antenna

VLF: Very Low Frequency; LF: Low Frequency; HF: High Frequency; VHF: Very High Frequency: UHF: Ultra High Frequency; SHF: Super High Frequency; EHF: Extremely High Frequency

Fig. 1. Various Categories of Antenna

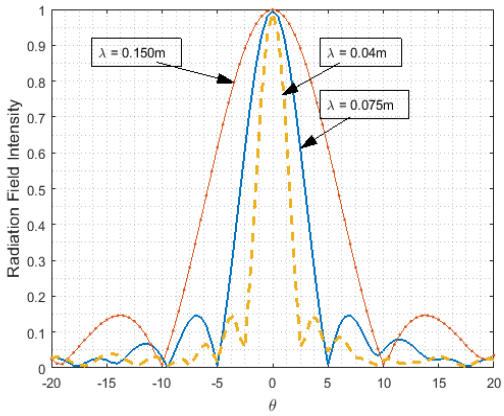

Fig. 2. Variation of bandwidth at different frequencies

2. Structural shape analysis of paraboloid shell

Finite Element (FE) analysis for the structure is performed using ABAQUS software. The parabolic geometry is meshed with 4-noded shell elements having six Degrees of Freedom (DoFs) at each node. Total number of 402 nodes and 373 elements are considered to perfectly model the deformation of the system and stress profile. It is analyzed that with a mesh of 402 elements, the degree of stress discontinuity between the adjacent nodes decreases significantly. These nodes are subdivided into 3 major sets namely (i). Actuated node set (ii) Fixed node set and (iii) Internal node set. Vertical forces of different magnitude are applied on various actuated nodes and deformed shape of antenna is analyzed. With the application of force at a Control Pont (CP) (see Fig.3), the inflation and deflation on antenna surface is shown in Fig.4. This shows the coupled behavior of a nodal position with neighboring nodes. Hence, in order to perform shape control the following procedure is adopted.
The undeformed nodal coordinates, stiffness matrix (K) containing material information of each node are exported from the FE software. After applying the fixed boundary conditions, the stiffness matrix is statically condensed using the Guyan reduction technique. For DoFs other than y-direction, all internal nodes and fixed nodes are eliminated. Subsequently, a direct mathematical relation between applied force (F), initial coordinates (x_{ini}) and deformed coordinates (x_{def}) is established as shown in equation (1).

$$F = K\left(x_{ini} - x_{def}\right) \quad (1)$$

2.1. Selection of SMA for shape control of antenna structure

In order to select an appropriate SMA actuator for the reflector, the stiffness contribution at individual CP of structure is measured by loading the CP using dead weights and measuring the deflection by the single point laser sensor. The force to deflection curve is shown in Fig.5, the ratio K (400N/m) is linear upto the deflection range of approximately 25mm. No major difference in the stiffness value at 8 CPs was recorded, as the structure was symmetric. This range of deflection is considered as elastic range. Based upon this stiffness value, heating and cooling force requirement, maximum displacement requirement on a CP, SMA wire of diameter 375µm was chosen.

2.2 Analysis of SMA actuator with constraint structure

For this application SMA wire is heated using Joule effect. Hence, a simple mathematical model is developed in which SMA is considered as a lumped body [6]. When electric current flows through it, it performs the mechanical work in addition to heat losses. As current flow stops it starts heat rejection. As the total energy of the system has to be conserved so one can equate the total electrical energy consumed by the actuator to work performed with some heat losses as shown in equation (2).

Since, the magnitude of heat losses due to radiation and conduction, latent heat and mechanical work is small (20%) in comparison to the other factors, hence equation (2) is simplified to equation (3). For multiple voltage inputs the analytical solution of (3) is given in equation (4). Where, T_a is the ambient temperature, t_F is the end time, t_I is the initial time period, A_i is the voltage amplitudes, t_i^e is the end time of voltage A_i, t_i^s is the start time of voltage A_i.

$$\underbrace{\frac{V^2(t)}{R}}_{\substack{Power\\supplied}} = \underbrace{hA(T(t)-T_a)}_{\substack{Convective\ heat\\loss}} + \underbrace{\sigma_{rad}A(T^4(t)-T_a^4)}_{Radiative\ heat\ loss} + \underbrace{\rho V c_p \frac{dT}{dt}}_{\substack{Specific\\heat}} + \underbrace{kA\frac{(T(t)-T_a)}{l}}_{\substack{conductive\ heat\\loss}} + \underbrace{\rho V \delta H \frac{d\xi}{dT}}_{\substack{Latent\\heat}} + \underbrace{\frac{dW_{mech}}{dt}}_{\substack{Mechanical\\work}} \tag{2}$$

$$\frac{V^2(t)}{R} = hA(T(t)-T_a) + \rho V c_p \frac{dT}{dt} \tag{3}$$

$$T = T_a + \frac{1}{e^{t_1 t_F} - e^{t_1 t_I}} \sum_i^n \frac{A_i^2}{\tau_1 \tau_2} (e^{\tau_1 t_i^e} - e^{\tau_1 t_i^s}) \tag{4}$$

where, $\tau_1 = \frac{\rho V c_p}{h_c A}, \tau_2 = \rho V c_p R_w$

Using Brinson model [7], the displacement at a CP is analyzed by incorporating the stiffness (K) in equation (5). The strain profile of a CP on the constraint structure actuated using SMA wire (diameter = 375µm) by applying voltage profile is shown in Fig.6. A direct mathematical relationship between the displacement of CP and temperatures of SMA wire is developed using rational polynomial algorithm in MATLAB. The relationship for heating cycle is shown in equation (6). This relationship covers the temperature range from 30°C to 100°C. Cooling cycle of SMA is not considered due to the presence of locking device that is discussed in section (Experimental setup).

$$\sigma - \sigma_0 = D(\xi)\epsilon - D(\xi_0)\epsilon_0 + \Omega(\xi_0)\xi_{s_0} + \Theta(T - T_0) + \frac{kx}{A} + \frac{kx_0}{A} \tag{5}$$

$$x = \frac{p_1 T^4 + p_2 T^3 + p_3 T^2 + p_4 T + p_5}{T^2 + q_1 T + q_2} \tag{6}$$

$$p_1 = 5.824e^{-7}; p_2 = -0.0003374; p_3 = 0.04289; p_5 = 26.84; q_1 = -154.6; q_2 = 6117$$

3. Shape optimization

The shape optimization of the antenna is formulated as a multi-objective optimization problem where, the optimization is performed by considering the eight CPs on the structure. The following objective functions are considered:

- Minimization of mean square error between the desired and current shape

- Minimum total voltage requirement to actuate the actuators

With a constraint that stress and strain in wire should not increase the safe stress of 180 MPa and 0.05% respectively. At the safe stress level effect of functional fatique can be neglected.

$SE = \frac{\epsilon^2 E}{2}$, strain ($\epsilon$) at temperature (T) where, $E = E_A + \xi(\mathrm{E_M} - \mathrm{E_A})$

Displacement error = $x_{desired}$ - x,

Mean square error, (MSE)= $\sqrt{x_{d_i}^2 - x_i^2}$

Power, $\frac{V^2}{R}$; $R = R_A + \xi(R_A - R_M)$

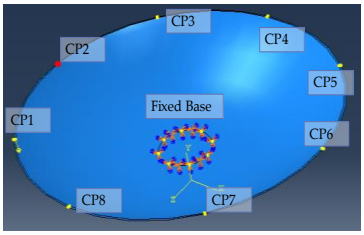

Fig.3. Eight Control Points on the structure

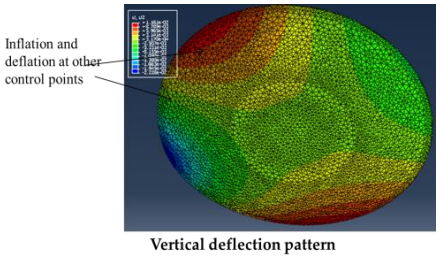

Fig.4. Inflation and deflation on structure while deforming a CP

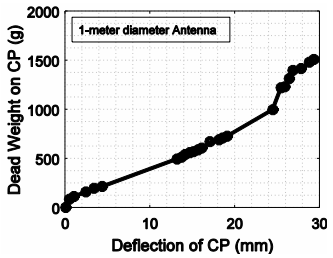

Fig.5. Experimental Result to calculate the stiffness at a CP

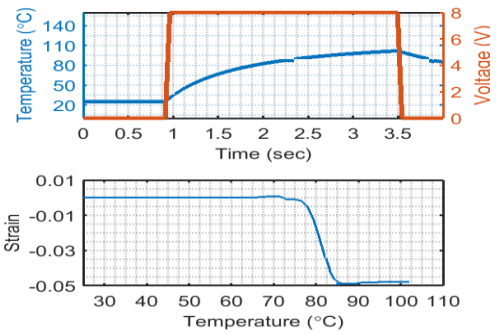

Fig.6. Displacement of a CP by heating SMA

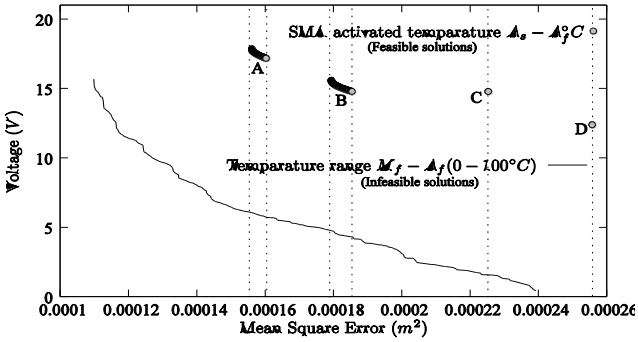

Fig.7. Non-dominated solutions between Mean Square Error versus Voltage for Case-I

The multi-objective optimization problem is solved using evolutionary multi-objective optimization. Constrained Non-dominated Sorting Genetic Algorithm-II (NSGA-II) [8] is used to solve the multi-objective optimization problem. The following parameters for are considered:

Population size = 40n, (n=Number of variables)
Number of Generations = 500,
SBX probability= 0.9,
SBX index = 10,
Polynomial mutation probability = 1/n, and
Mutation index = 100

Two different cases of the parabolic space antenna are considered commonly known as steering and shaping. For Case-I, a desired displacement array of (250, -120, -100, 250, -100, 200, -60, 140)µm and for case-II desired array displacement of (250, -50, -50, 0, 200, 0, -50, -80)µm at CP1-8 is considered. The non-dominated solutions between mean square error versus voltage is shown in Fig.7. The shape of the Pareto-front is non-convex. Due to the presence of non-linearity classical weighted sum approach is unable to generate non-dominated solutions [9]. The figure clearly shows that a better set of non-dominated solutions (both in terms of mean square and voltage) can be obtained for the temperature range between M_s to A_f i.e between (52−100°C). However, the actuating temperature of

SMA is between A_s to A_f (70−100°C) including various constraint recovery stresses. This is the reason for the infeasibility of all those solutions ranging between M_f to A_f . All those solutions having temperature below 70°C will not be actuated. As a result, the feasible range for all temperatures must lie between 70−100°C. The figure also shows that the range of mean square error is between 156 μm to 256μm and the voltage ranges from 12.39 to 17.86V. For minimum mean square solution temperature at first actuator should be 92.74°C, temperature at the fourth actuator should be 70°C and all other temperature must be zero. On the other hand, for minimum voltage solution all the temperature must be zero. The meaning is that there will not be any movement of the antenna.

The change in temperature range will change the non-dominated solutions. Multi-objective optimization method works with two different spaces i.e. variables space and objective space. The temperature range between (A_s to A_f) has reduced the feasible region in the variable space which has been restricted the objective space. The feasible solutions has four different zones shown with A, B, C and D. All solutions in these zones have equal importance.

The range of mean square error is ranging from 37μm to 145μm whereas minimum voltage is 12.39V and maximum voltage is 18V. Temperature at first actuator should be 97°C, sixth actuator temperature should be 70°C and all other actuator temperature should be zero to obtain minimum mean squared error solution. However, all the temperature must be zero to achieve minimum voltage solution. If a user wants to use minimum value of mean square error, the left most solution in zone A must be chosen. On the other hand for lowest voltage solution D will be choice. We will analyse the effect of temperature in each objective function in next subsection.

The Pareto-optimal solutions for case-II can be seen in Fig.8. A better mean squared error solutions has been obtained in Case-II as compared to Case-I. Case-II also contains four zones like Case-I. The comparison between case-I and Case-II has been shown in Fig.9. The figure clearly shows that the obtained solutions are better in both objective functions in Case-II than Case-I.

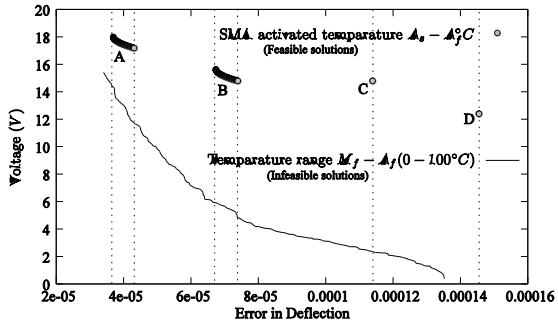

Fig.8. Non-dominated solutions between Mean Square Error versus Voltage for Case-II

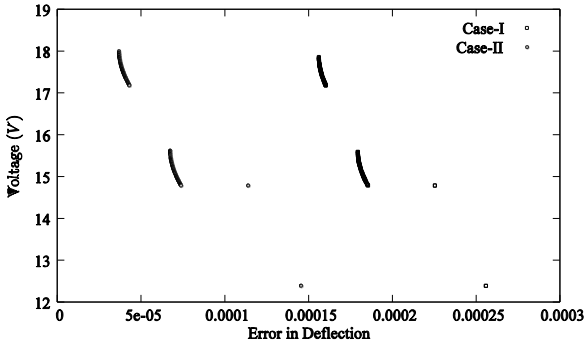

Fig.9. Comparison of non-dominated solutions between Mean Square Error versus Voltage for both cases

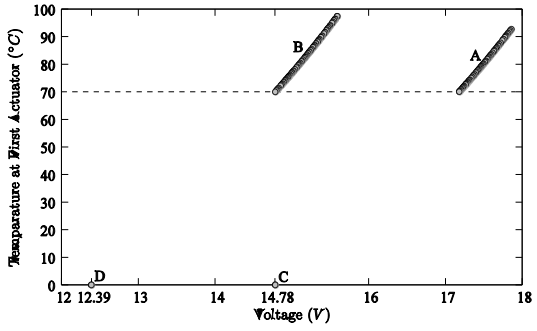

Fig.10. Relationship between Voltage with temperature of First Actuator for Case-I

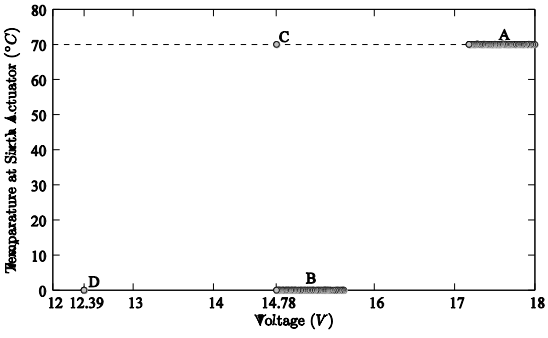

Fig.11. Relationship between Voltage with temperature of Sixth Actuator for Case-II

Fig.12. Experimental setup of Reconfigurable parabolic antenna

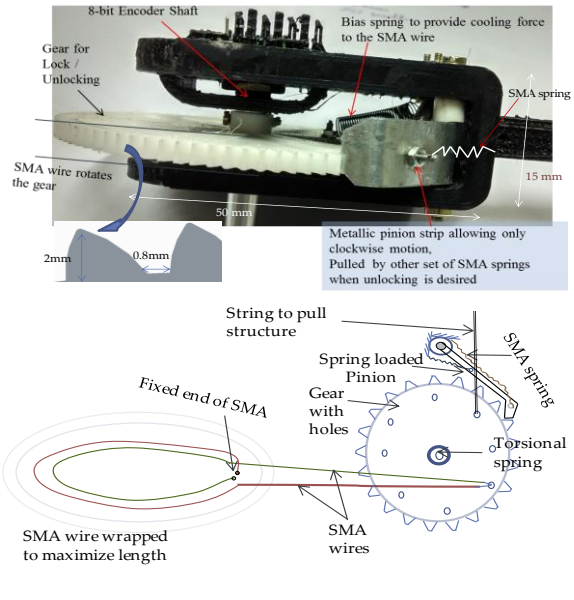

Fig.13 (a). Locking device (b) A schematic of SMA wire wrap around antenna with locking device working demonstration

3.1 Temperature effect in objective functions

Here, we analysed the effect of temperature in both the objective functions i.e. mean square error and voltage. As mean square error and voltage are conflicting to each other, the relationship with any one of the objective functions with temperature is sufficient. The other will follow inverse relationship. Here, we use voltage to establish a relationship between temperatures of different actuators.

Fig.10 shows the relationship between temperatures of the first actuator versus voltage. Here we can see four different relationships exist. These four zones have been marked with A, B, C and D. These four zones are nothing but four zones of non-dominated solution shown in Fig.7. In A and B zone voltage is direct proportional to temperature which means that if we want an increase in voltage temperature must be increased and vice versa. For zones C and D temperature should be kept at ambient temperature (T_a).

Similar to the first actuator, the relationships of other actuators is developed. A user has to keep the temperature at 70^{o}C to achieve a solution in A and C zones. On the other hand, to achieve voltage at zones B and D, the temperature must be kept at T_a. The relationships between voltage and actuator temperature for Case-II is shown is Fig.11. User can vary the temperature to obtain voltage accordingly. This relationship will help the decision maker to take decision by varying the temperature based on desired voltage.

4. Experimental setup

The parabolic reflector setup with single feed mount is shown in Fig.12. The CPs are actuated using auto locking device as shown in Fig.13(a). One end of the SMA wire is fixed with the base of the reflector and the other end rotates the geared pulley mounted at the fixed platform as shown in Fig. 13(b). The working principle of the locking mechanism developed in this work is similar to the ratchet mechanism in which a metallic strip (pinion) being pulled by bias spring that allows only anti-clockwise rotation of the pulley. When unlocking is desired, the pinion can be pulled using SMA spring. In order to keep the shaft rotation frictionless, roller bearings are used. For sensing the shaft rotation, an 8 bit absolute encoder with 128 pulse per revolution is mounted with the shaft of pulley. The digital data are fed into the controller, which using a PID control algorithm decides the power supply required to the SMA actuators. The block diagram of the closed loop controller is shown in Fig.14.

4.1 EM Simulation results

The deformed mesh from ABAQUS is converted to surface thereafter EM software package High Frequency Structure Simulator (HFSS) and MATLAB are exclusively used to generate the EM patterns. The results of radiation pattern for deformed and un-deformed Antenna geometry is shown in Fig.15, 16. The results clearly show the shifting of major lobe of EM pattern. This shifting can be very useful for the EM analysts. The following advantages can be undertaken using the shift:

- Two beam modes, steering and shaping can be predominately achieved using this system. Hence, in space by using reconfigurable antennas system bigger landmasses, different landmasses can be covered.
- Recovery of manufacturing errors, in orbit thermal distortion, loosed structural joints, material degradation, creep can be compensated with this technology.
- The precise antenna surface control for beam broadening applications, can be easily achievable using reconfigurable antenna. The major advantage of such systems is in the field of radio astronomy.
- With similar system researchers at Ohio state University [3] successfully demonstrated beam steer from the North America to South America.

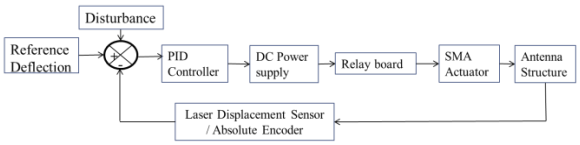

Fig.14. Closed Feedback control loop for Antenna

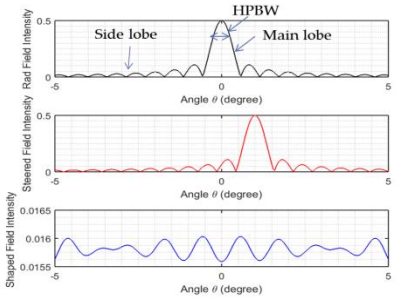

Fig.16 Far field intensity for the analysis of deformed Antenna using MATLAB

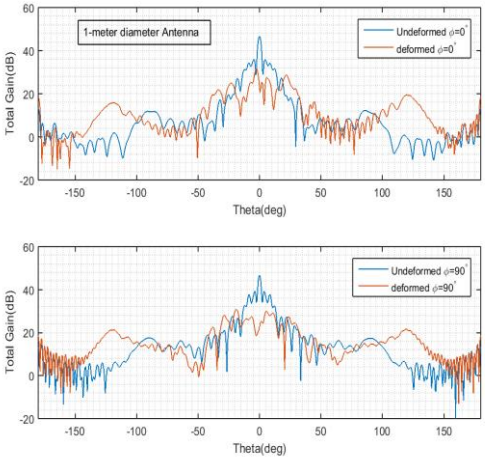

Fig.15 EM pattern for un-deformed and deformed geometry at $\phi = 0,90^{o}$ using HFSS

5. Conclusion and future scope

The feasibility of shape control of RF reflector using SMA based actuation system is demonstrated in this paper. The steering and shaping modes of EM pattern can be useful in space for coverage of larger or different landmasses at the same time. As a Proof-of-Concept model, the present antenna structure has to be verified under Compact Antenna Test Facility (CATF) of ISRO, so that the Design Validation can be established for space worthy hardware in near future. This approach has potential applications in ground segment and Air Borne systems as well, which are being explored by the authors.

6. References

[1] Landeros S., Neri R., Samano R., *A Tutorial on the Synthesis of Single Shaped Reflectors in C, KU, and KA Bands* Taylor and Francis 26(2), p. 131–154, (2006)

[2] Cherrette, A. R., Lee S W., Acosta R J., *A Method for Producing a Shaped Contour Radiation Pattern Using a Single Shaped Reflector and a Single Feed*, IEEE Transactions on Antennas and Propagation 37(6), p. 698-706, (1989)

[3] H. Yoon, Design, Modeling, and Optimization of a Mechanically Reconfigurable Smart Reflector Antenna System, PhD dissertation, The Ohio State University, (2002)

[4] Chawla, A., Bhattacharya, B., and Munjal, B. S., *Optimal Actuation of SMA-Wire Network for*

Adaptive Shape Control of a Space Antenna System, Proceedings in IEEE, ICARCV, Singapore, (2014)

[5] Kalra, S., Bhattacharya, B., and Munjal, B. S., *Design of shape memory alloy actuated intelligent parabolic antenna for space applications*, Smart Material and Structures, IOP Science, vol.26(9) (2017)

[6] Meier, H. and Oelschlaeger, L., *Numerical thermomechanical modelling of shape memory alloy wires*, Materials Science and Engineering A, Elsevier vol. 378, p. 484–489, (2004)

[7] Brinson, L. C., One Dimensional Constitutive Behavior of Shape Memory Alloys: Thermomechanical Derivation With Non-Constant Material Functions and Redefined Martensite Internal Variable, Journal of intelligent material systems and structures, vol. 4, no. 2, p. 229–242, (1993).

[8] Deb, K., Pratap, A., Agarwal, S. and Meyarivan, T., *A fast and elitist multiobjective genetic algorithm: NSGA-II*, IEEE Transactions on Evolutionary Computation, vol. 6, no. 2, p. 182–197, (2002)

[9] Deb, K., *Multi-Objective Optimization using Evolutionary Algorithms*, handbook, John Wiley & Sons, ISBN: 978-0-471-87339-6, (2001)